Hindawi Publishing Corporation
Journal of Geological Research
Volume 2011, Article ID 946701, 18 pages
doi:10.1155/2011/946701

Research Article

The Cretaceous Alkaline Dyke Swarm in the Central Segment of the Asunción Rift, Eastern Paraguay: Its Regional Distribution, Mechanism of Emplacement, and Tectonic Significance

Victor F. Velázquez,[1] Claudio Riccomini,[2] Celso de Barros Gomes,[2] and Jason Kirk[2]

[1] *Escola de Artes, Ciências e Humanidades, Universidade de São Paulo, Rua Arlindo Béttio 1000, Ermelino Matarazzo, 03828-000 São Paulo, SP, Brazil*
[2] *Instituto de Geociências, Universidade de São Paulo, Rua do Lago 562, 05508-080 São Paulo, SP, Brazil*

Correspondence should be addressed to Victor F. Velázquez, vvf@usp.br

Received 21 July 2010; Revised 16 November 2010; Accepted 19 February 2011

Academic Editor: Jan Veizer

A structural analysis of Cretaceous alkaline dykes swarm associated with the central segment of the Asunción Rift is reported here. Dykes are generally single near-vertical tabular bodies, less than 5 m wide, although multiple and composite intrusions also occur. Many of these small bodies have been emplaced into Paleozoic sedimentary rocks and exhibit a regional NW-SE orientation pattern. Petrographical and geochemical data allow recognition of two different lineages of potassic dykes: a silica-undersaturated suite ranging from basanite to phonolite (B-P) and a silica-saturated suite ranging from alkali basalt to trachyte (AB-T). The morphological features, the regional en-échelon distribution, and the NW-SE orientation pattern suggest that the dykes were injected along fractures and faults, under a transtensional tectonic regime with $\sigma 1$ NW/horizontal, $\sigma 2$/vertical, and $\sigma 3$ NE/horizontal. Detailed analysis, combining dyke petrography, orientation pattern, and relative chronology reveals a rotation from WNW toward NNW during dyke emplacement. In terms of the paleostress field orientation, the evidence indicates that the dykes were diachronically formed under a similar stress condition. Finally, the pattern of orientation documented for the Cretaceous alkaline dykes of the Asunción Rift is consistent, temporally and spatially, with the phases of regional deformation that occurred during the process of the Atlantic Ocean opening.

1. Introduction

In many volcanic systems, dyke intrusions of variable size and composition are often considered the main channel feeders and represent one of the more important vertical transfer routes of mantle-derived molten material through the lithosphere to the upper crust. In general, dykes occur in diverse geological times and tectonic settings; however, the vast majority of the dyke swarms on continental areas are of the Proterozoic or Late Phanerozoic age [1]. Although their abundance in the crust is less expressive than continental flood basalts and large granitic masses, dykes are excellent tracers for many geological processes. Over the last two decades, numerous geochemical studies have been carried out on these small vertical tabular-like bodies with the purpose of better understanding the cause and nature of partial melting and magmatic differentiation processes. Consequently, many of the predictions made about the thermodynamic behavior and the conditions that govern the lower and upper mantle are based on the isotope and trace element signatures of dykes [2–4]. Dykes are largely used to examine the relationship involving elastic brittle-fluid-host rocks and magma transport. These studies are mainly targeted at determining the regional paleostress fields and the active mechanism [4, 5]. A theoretical and applied approach about the emplacement mechanism and propagation of individual dykes is well documented in the synoptic paper of Anderson [6].

Eastern Paraguay is an intracratonic region situated in the westernmost border of the Paraná basin. During Early to Late Cretaceous time, this region was affected by an important tectonomagmatic event, the Paraná-Etendeka

large igneous province (cf. [7]) related to the opening of the South Atlantic Ocean, which caused a series of alkaline magmatic episodes [8, 9]. Although the distribution of these alkaline bodies is quite widespread around the Paraná basin (Figure 1), in the Eastern Paraguay region, they are confined to distinct well-exposed areas. In the northern (Rio Apa) and northeastern (Amambay) provinces, the alkaline rocks show similar ages of 138.9 ± 0.7 Ma (cf. [10]), predating the tholeiitic lavas of the Serra Geral Formation (133–130 Ma, cf. [11–15]). However, in the Central-Eastern (Central) and southern (Misiones) provinces, they are younger than the basaltic rocks, 126.4 ± 0.4 Ma and 118.3 ± 1.6 Ma, respectively (cf. [10]).

One of the most conspicuous occurrences of alkaline rocks in Eastern Paraguay is represented by the Central Province. Geological and geophysical data indicate that the Asunción Rift development, in Cretaceous time, was responsible for multiple diachronous events of potassic alkaline magmatism (Central Province, cf. [10, 16, 17]). The mode of occurrence of the numerous bodies is quite variable. Intrusive formations are mainly represented by stocks of various dimensions; on the other hand, the extrusive units comprise essentially lava flows, domes, and plugs. Nevertheless, the most significant magmatic event of the province is represented by the hypabyssal rocks, occurring largely as individual dykes, which exhibit a wide variation in composition, texture, and size.

The good exposure of the outcrops offers an excellent opportunity to examine in detail the contact relationships, the morphological feature of the walls surface, and the orientation pattern of the dykes. Based on these data, this paper discusses the mechanism of emplacement, as well as the regional distribution of the paleostress field at the time of intrusion.

2. Geological Setting

The central area of Eastern Paraguay is characterized by an important tectonomagmatic-sedimentary event of Early Cretaceous age [18–20]. The major faulting zone is represented by the Asunción Rift [21], a tectonic feature of roughly 200 km length and 25–45 km wide, with NW-SE general orientation (Figure 2). According to Velázquez et al. [17] and Riccomini et al. [22], the rift consists of three different segments. The western segment, with a well-defined NW-SE-trend, extends more than 90 km between the localities of Benjamin Aceval and Paraguarí, and it comprises an extensive Cenozoic sedimentary deposit and several Tertiary intrusive bodies of sodic ultra-alkaline rocks (Asunción Province, cf. [17, 20, 23]). The central E-W-trending segment measures approximately 70 km, extends from the town of Paraguarí to the locality of Villarrica, and represents the region of major potassic alkaline magmatism. Largely, those rocks cut siliciclastic deposits of Silurian and Permian ages and locally the Early Cretaceous aeolian deposits of the Misiones Formation. Finally, the less defined NW-SE-trending eastern segment, with about 40 km of extension, is developed from the locality of Villarrica until the Ybytyruzú mountains. In the last area, the potassic alkaline rocks intrude both the Cretaceous aeolian deposits of the Misiones Formation and the overlying tholeiitic flows of the Paraná basin volcanism.

From a geodynamic viewpoint, at least two tectonic episodes of importance led to the current shape of the relief in the area. The first event, of Early Cretaceous age, which was induced by an NE-SW extensional tectonic regime, provoked major graben faulting and expressive potassic alkaline magmatism. The second one was also of extensional regime, with the major period of faulting taking place in the Paleocene. However, it continues until today causing small seismic movements of low amplitude in the region [24]. Possibly, a generalized lithospheric thinning and the emplacement of a hot mantle closer to the upper crust were responsible for the significant changes of the geothermic gradient occurred in this epoch. A detailed study of fission tracks in Silurian deposits and Cretaceous alkaline rocks (cf. [25]) indicates two different periods of thermal activity for the whole area, between 90–60 Ma and 60–10 Ma. These cooling ages are significantly younger than the tectonomagmatic event of the Central Province, but, in part, are consistent with the intrusion of the nephelinitic alkaline rocks of the Asunción Province, which mainly formed at 58.7 ± 2.4 Ma (cf. [10]). According to Riccomini et al. [20], the last period of time corresponds to an important tectonic phase, with generation of deep faulting that served as conduit for the mantle material to migrate to the surface of the crust.

3. Morphology, Occurrence and Field Relations

The potassic alkaline dyke intrusions are well exposed throughout a large section of the central segment of the Asunción Rift. More than 200 bodies of mafic, intermediate, and felsic dykes are randomly distributed in that region. The largest continuous exposures of individual dykes are found in the Sapucai district [16, 26] (Figure 3). Other important outcrops are confined to near the villages of Potero Ybaté and Gral. Bernardino Caballero is not so far from the town of Sapucai. Some dykes were also recorded in the Ybytymí region.

Most of the dykes show a continuous tabular aspect or are composed of several separate segments, resulting in an apparent sinuous intrusion. In both cases, they occur essentially as single intrusions, but multiple and composite injections are also present. Here, the multiple term is used to characterize a repeated injection of dyke with the same or similar compositions (alkaline basalt, trachybasalt, and trachyandesite), and composite when the repeated injections are of different compositions (alkaline basalt, tephrite, and phonolite).

The width of the dykes can vary from 0.15 m to 10 m, but in most of the cases is between 0.30–3 m; in general, the length cannot be traced for more than a few kilometers. Regionally, the dykes cross-cut Paleozoic deposits. In the Sapucai and Potrero Ybaté regions, they are intruded into lavas and plugs of alkaline rocks. The dyke-wall rock contact is usually vertical to subvertical, with chilled margins

well preserved, and with prevalence for normal dilatation. Oblique relative displacement between the walls, in a dextral or sinistral sense, was also observed.

In a regional distribution, the dykes show a parallel to subparallel orientation and, in some cases, an en-échelon arrangement (Figure 3). However, there are localities where the orientation is less regular, indicating a significant change of direction and trajectory. In this case, the intrusion relationship is complex. Dykes of distinct composition and generation display oblique and/or perpendicular intersections.

4. Nature and Composition

The main petrographical and geochemical features of the dykes have been extensively discussed by many authors [16, 18, 26–29], and the relevant features are summarised here.

Petrographical parameters (mineralogical assemblage and texture) and field relations (relative chronology of events and spatial distribution) allow recognition of three compositionally types of dykes showing distinct relationship: (a) *tephritic* (basanites-tephrites-tephriphonolites), (b) *phonolitic* (phonolites-peralkaline phonolites), and (c) *basaltic* (alkaline basalts-trachybasalts-trachyandesites-trachytes/trachyphonolites). The first two types are geochemically grouped together forming the B-P (basanite-phonolite) suite, whereas the third one into the AB-T (alkali basalt-trachyte) suite. Mineralogical and petrographical data reported in Comin-Chiaramonti et al. [18, 26] and Cundari and Comin-Chiaramonti [30] show that these rocks are usually porphyritic in texture, the groundmass being fine-grained or even aphyric and variable from holocrystalline to hyaline. Phenocrysts (mega and micro) are mainly represented by olivine, clinopyroxene, feldspars, (plagioclase and alkali feldspar) and feldspathoids; occasionally amphibole, biotite, garnet, and sphene can also be found. Some other general mineralogical features are: clinopyroxene composition (diopside to ferrosalite) consistently yielding Al enrichment trends; $Fo_{81–69}$ content of the olivine in tephrites and alkali basalts decreasing up to 65% in phonolites; zoned megacrysts of hastingsitic hornblende (core) to kaersutite (rim), associated with accessory groundmass pargasite in tephrites and phonotephrites; K-rich hastingsite and K-rich ferropargasite in phonolites; accessory groundmass mica (annite-phlogopite series), consistently yielding insufficient (Si+Al) to satisfy the T site position; phenocryst, that is, xenocrystal plagioclase $An_{70–20}$ and $An_{74–42}$ in tephrites and phonolites, respectively; coexisting plagioclase ($An_{14–22}$) microlites associated with soda-sanidine and sanidine; feldspathoids include analcimized leucite and nepheline; Ti-magnetite, rarely ilmenite or hematite, as Fe-Ti oxides; and Ti-andradite and sphene as main accessory minerals.

The mineralogical assemblage of the *tephritic-type* includes phenocrysts of clinopyroxene ($Wo_{40–50}Fs_{10–19}$), olivine ($Fo_{60–85}$) and leucite pseudomorphs (sanidine + nepheline) all set in a glassy groundmass consisting of microlites of clinopyroxene ± olivine, Ti-magnetite ± ilmenite, Ti-phlogopite-biotite, alkali feldspar ($Or_{15–88}$), and nepheline-analcime ($Ne_{44–59}Ks_{17–26}$). Plagioclase (up to An_{74}) is also present as phenocrysts in some samples. Accessory phases are amphibole (pargasite-kaersutite), apatite, and zircon. The *phonolitic-type* is characterized by phenocrysts of alkali feldspar ($Or_{47–75}$), leucite pseudomorphs, clinopyroxene ($Wo_{48–50}$), ferropargasite, nepheline ± biotite ± sphene ± melanite (Ti-andradite up to 68%) ± magnetite, or hematite. Glassy groundmass has alkali feldspar, nepheline, and clinopyroxene ± melanite ± opaques microlites. The composition of the *basaltic-type* for the alkali basalts, trachybasalts, and trachyandesites shows pheno and/or microphenocrysts of clinopyroxene ($Wo_{44–49}Fs_{7–15}$), olivine ($Fo_{65–83}$), plagioclase ($An_{28–76}$), magnetite, and biotite. The glassy groundmass contains microlites of clinopyroxene ($Wo_{46–49}Fs_{13–18}$), magnetite, ilmenite, biotite, plagioclase ($An_{20–45}$), alkali feldspar ($Or_{52–65}$), nepheline-analcime ($Ne_{37–73}Ks_{22–38}$), amphibole, and apatite ± sphene ± zircon. On the other hand, the mineralogy for the trachyphonolites and trachytes includes phenocrysts of alkali feldspar ($Or_{60–65}$), clinopyroxene ($Wo_{46–49}Fs_{14–20}$), plagioclase ($An_{14–16}$), leucite pseudomorphs, amphibole, and biotite in hypocrystalline to glassy groundmass having microlites of alkali feldspar, biotite, and clinopyroxene ± biotite ± amphibole ± magnetite ± Ti-andradite ± hematite.

Geochemical analyses and Sr-Nd isotopic signatures indicate that the dykes are quite variable in composition. Gomes et al. [31] and Comin-Chiaramonti et al. [26, 28], using chemical data of minerals and bulk rocks and petrochemical classification, grouped all the potassic dykes into two main lines of evolution: (a) a silica-undersaturated lineage ranging from basanite to phonolite (B-P) and (b) a silica-saturated lineage ranging from alkaline basalt to trachyte (AB-T) (Figure 4), probably related to distinct parental magmas. In general, both suites show similar elemental enrichment patterns for large ion lithophile elements (LILE), that is, Rb and Ba, as well as for other incompatible elements, such as La, Ce, Sm, and Tb. Nevertheless, the major differences between the two groups are the higher concentrations of K_2O, TiO_2, Zr, Nb, Y, and REE of the B-P rocks in comparison to those of the AB-T suite. Mg-values (Mg*) and Ni and Cr contents indicate that all the magma-types representative of the less evolved dykes in the investigated area can be considered to some extent to be derivatives [26].

Subsequent researchers have been seeking to establish the mechanism of generation and evolution of the alkaline magmatism in Central-Eastern Paraguay. Based on textural, mineralogical and petrochemical evidence and utilizing quantitative mass balance calculations on major oxides, the latter authors [8, 18] concluded that fractional crystallization was a potentially important process in the formation of these rocks. Furthermore, Sr and Nd isotope data suggested that the parental magmas responsible for the alkaline potassic series (B-P and AB-T) and sodic suites occurrences, found in some areas of Eastern Paraguay (northern, central, and southern: Alto Paraguay, Asunción, and Misiones provinces, respectively (cf. [10]), would have derived from a heterogeneous subcontinental mantle lithospheric source, submitted to different melting degrees and variously enriched in

Table 1: Additional information about the alkaline dykes that occur in the central segment of the Asunción Rift.

Field number	Latitude/Longitude	Dip direction	Width (m)	Rock	Evolutive trend	References	Chronology
001	25°40′53″ S/56°56′36″ W	355/89	1.30	Trachybasalt	AB-T	[8, 21, 36]	
002	25°41′31″ S/56°56′34″ W	342/89	1.40	Tephriphonolite	B-P	This paper	
003	25°41′34″ S/56°56′32″ W	150/89	0.40	Phonolite	B-P	This paper	
004	25°41′08″ S/56°56′41″ W	320/89	1.00	Tephriphonolite	B-P	[8, 21, 36]	
005	25°41′34″ S/56°56′55″ W	130/89	0.70	Phonolite	B-P	This paper	
006	25°41′40″ S/56°56′58″ W	145/89	0.90	Phonotephrite	B-P	This paper	
007	25°41′58″ S/56°56′18″ W	170/89	1.70	Phonolite	B-P	This paper	
008	25°41′50″ S/56°56′51″ W	325/89	1.45	Tephrite	B-P	This paper	
009	25°42′14″ S/56°56′48″ W	310/89	1.30	Phonotephrite	AB-T	This paper	
010	25°41′45″ S/56°56′19″ W	305/89	0.45	Trachybasalt	AB-T	This paper	10 is cut by 11
011	25°41′55″ S/56°56′19″ W	130/89	0.80	Tephriphonolite	B-P	This paper	
012	25°41′58″ S/56°56′01″ W	320/89	0.70	Trachyandesite	AB-T	[8, 21, 36]	
013	25°42′11″ S/56°57′04″ W	092/89	0.60	Peralk. Phon.	B-P	This paper	
014	25°42′25″ S/56°57′06″ W	290/89	1.00	Trachyte	AB-T	[8, 21, 36]	
015	25°42′39″ S/56°57′09″ W	075/89	0.50	Peralk. Phonol.	B-P	[8, 21, 36]	
016	25°42′56″ S/56°57′11″ W	042/89	1.20	Tephrite	B-P	[8, 21, 36]	
017	25°42′58″ S/56°57′19″ W	287/89	0.80	Alkali basalt	AB-T	This paper	
018	25°42′58″ S/56°57′19″ W	020/89	1.00	Trachyandesite	AB-T	This paper	
019	25°43′20″ S/56°57′15″ W	075/89	0.50	Phonolite	B-P	This paper	
020	25°45′57″ S/56°57′27″ W	065/89	0.90	Phonolite	B-P	This paper	
021	25°45′59″ S/56°57′30″ W	325/89	0.35	Trachybasalt	B-P	[8, 21, 36]	
022	25°45′59″ S/56°57′30″ W	340/89	0.20	Phonotephrite	B-P	This paper	
023	25°44′29″ S/56°57′36″ W	055/89	0.70	Tephrite	B-P	This paper	
024	25°44′29″ S/56°57′36″ W	045/89	0.80	Phonotephrite	B-P	This paper	
025	25°39′45″ S/56°58′11′ W	140/89	1.30	Tephriphonolite	B-P	This paper	25 is cut by 26
026	25°39′50″ S/56°58′13′ W	310/89	0.25	Phonolite	B-P	[8, 21, 36]	
027	25°39′50″ S/56°57′40′ W	110/89	0.20	Trachyandesite	AB-T	[8, 21, 36]	
028	25°40′06″ S/56°57′44″ W	130/89	0.40	Tephriphonolite	B-P	This paper	
029	25°40′05″ S/56°57′41″ W	110/89	0.60	Trachybasalt	B-P	This paper	
030	25°40′09″ S/56°57′30″ W	310/89	0.25	Tephrite	B-P	This paper	
031	25°40′10″ S/56°57′37″ W	165/89	0.35	Peralk. Phon.	B-P	[8, 21, 36]	
032	25°40′17″ S/56°57′42″ W	118/89	2.40	Trachy	AB-T	[8, 21, 36]	32 is cut by 31
033	25°40′27″ S/56°57′40″ W	140/89	0.35	Phonotephrite	B-P	[8, 21, 36]	
034	25°40′30″ S/56°57′46″ W	330/89	1.20	Tephriphonolite	B-P	This paper	
035	25°40′32″ S/56°57′43″ W	130/89	0.25	Tephrite	B-P	This paper	
036	25°40′35″ S/56°57′40″ W	120/89	0.40	Trachyte	AB-T	This paper	
037	25°40′37″ S/56°57′39″ W	140/89	0.15	Tephriphonolite	B-P	This paper	
038	25°40′39″ S/56°57′43″ W	290/89	1.00	Trachyandesite	AB-T	This paper	
039	25°40′40″ S/56°57′35″ W	310/89	0.35	Phonotephrite	B-T	This paper	
040	25°40′41″ S/56°57′30″ W	165/89	0.40	Phonolite	B-P	[8, 21, 36]	
041	25°40′40″ S/56°57′50″ W	310/89	0.15	Phonotephrite	B-P	[8, 21, 36]	
042	25°40′42″ S/56°57′55″ W	290/89	0.25	Trachyandesite	AB-T	This paper	
043	25°40′53″ S/56°57′32″ W	330/89	0.40	Tephriphonolite	B-P	This paper	
044	25°40′56″ S/56°57′30″ W	130/89	0.20	Tephriphonolite	B-P	This paper	44 is cut by 45
045	25°40′56″ S/56°57′30″ W	320/89	1.50	Peralk. Phon.	B-P	This paper	
046	25°41′02″ S/56°57′40″ W	330/89	0.35	Tephrite	B-P	This paper	
047	25°41′09″ S/56°57′30″ W	320/89	0.15	Phonolite	B-P	This paper	
048	25°41′08″ S/56°57′47″ W	160/89	0.40	Phonotephrite	B-P	This paper	
049	25°41′12″ S/56°57′52″ W	145/89	2.00	Tephrite	B-P	[8, 21, 36]	
050	25°41′17″ S/56°57′42″ W	300/89	0.45	Trachybasalt	AB-T	This paper	

Table 1: Continued.

Field number	Latitude/Longitude	Dip direction	Width (m)	Rock	Evolutive trend	References	Chronology
051	25°42′23″ S/56°58′10″ W	310/89	0.35	Peralk. Phon.	B-T	[8, 21, 36]	
052	25°42′26″ S/56°58′19″ W	140/89	0.90	Tephriphonolite	B-P	This paper	
053	25°41′20″ S/56°58′25″ W	070/89	2.30	Phonolite	B-T	[8, 21, 36]	
054	25°39′41″ S/56°58′35″ W	130/89	0.45	Phonotephrite	B-P	[8, 21, 36]	
055	25°39′42″ S/56°58′30″ W	165/89	0.70	Peralk. Phon.	B-P	[8, 21, 36]	
056	25°40′17″ S/56°57′31″ W	130/89	0.35	Trachyandesite	AB-T	This paper	
057	25°39′55″ S/56°58′11″ W	150/89	1.00	Tephrite	B-P	[8, 21, 36]	
058	25°39′35″ S/56°58′36″ W	657/89	1.20	Tephriphonolite	B-P	[8, 21, 36]	
059	25°40′37″ S/56°58′34″ W	285/89	0.60	Trachyte	AB-T	[8, 21, 36]	
060	25°40′43″ S/56°58′42″ W	050/89	0.80	Trachy	AB-T	[8, 21, 36]	
061	25°41′10″ S/56°58′39″ W	335/89	1.20	Phonotephrite	B-P	[8, 21, 36]	
062	25°41′10″ S/56°58′39″ W	135/89	1.00	Peralk. Phon.	B-P	[8, 21, 36]	
063	25°41′24″ S/56°59′09″ W	285/89	0.70	Trachyandesite	AB-T	[8, 21, 36]	63 is cut by 62
064	25°41′49″ S/56°59′57″ W	070/89	1.40	Phonolite	B-P	[8, 21, 36]	
065	25°41′24″ S/56°58′36″ W	060/89	3.50	Tephrite	B-P	[8, 21, 36]	
066	25°42′48″ S/56°58′59″ W	050/89	2.20	Tephrite	B-P	[8, 21, 36]	
067	25°42′50″ S/56°58′56″ W	315/89	0.20	Phonolite	B-P	This paper	
068	25°42′53″ S/56°58′35″ W	320/89	0.15	Trachyte	AB-T	This paper	
069	25°42′55″ S/56°58′45″ W	330/89	0.40	Peralk. Phon.	B-P	[8, 21, 36]	
070	25°42′43″ S/56°58′53″ W	230/89	1.00	Tephriphonolite	B-P	[8, 21, 36]	
071	25°41′22″ S/56°55′20″ W	260/89	4.00	Phonotephrite	B-P	This paper	
072	25°41′25″ S/56°55′15″ W	130/89	0.25	Peralk. Phon.	B-T	This paper	
073	25°41′36″ S/56°55′10″ W	140/89	0.15	Tephrite	B-P	This paper	
074	25°41′39″ S/56°55′04″ W	125/89	3.50	Phonolite	B-P	This paper	
075	25°41′42″ S/56°55′10″ W	330/89	0.20	Tephriphonolite	B-P	[8, 21, 36]	
076	25°42′01″ S/56°54′59″ W	340/89	0.35	Phonolite	B-P	[8, 21, 36]	
077	25°42′01″ S/56°54′59″ W	110/89	1.40	Trachyte	AB-T	This paper	
078	25°42′06″ S/56°54′53″ W	330/89	0.30	Phonolite	B-P	This paper	
079	25°42′37″ S/56°54′47″ W	150/89	0.40	Tephriphonolite	B-P	This paper	
080	25°42′43″ S/56°55′03″ W	335/89	3.20	Tephrite	B-P	This paper	
081	25°42′06″ S/56°52′26″ W	075/89	2.30	Peralk. Phon.	B-P	This paper	
082	25°42′18″ S/56°56′03″ W	305/89	0.25	Trachyte	AB-T	[8, 21, 36]	
083	25°42′20″ S/56°52′35″ W	230/89	0.40	Tephriphonolite	B-P	[8, 21, 36]	
084	25°42′21″ S/56°52′37″ W	050/89	5.00	Tephriphonolite	B-P	This paper	
085	25°42′40″ S/56°53′29″ W	140/89	0.35	Tephrite	B-P	This paper	
086	25°42′57″ S/56°53′39″ W	310/89	0.15	Tephrite	B-P	This paper	
087	25°43′02″ S/56°53′19″ W	065/89	1.50	Phonolite	B-P	This paper	
088	25°42′22″ S/56°53′35″ W	300/89	0.30	Tephriphonolite	B-P	This paper	
089	25°42′25″ S/56°53′33″ W	345/89	0.25	Phonolite	B-P	This paper	
090	25°42′29″ S/56°53′39″ W	230/89	10.0	Trachybasalt	AB-T	This paper	90 is cut by 91
091	25°42′29″ S/56°54′39″ W	330/89	0.35	Tephrite	B-P	This paper	
092	25°42′40″ S/56°54′12″ W	150/89	0.25	Phonolite	B-T	This paper	
093	25°43′02″ S/56°54′20″ W	110/89	2.20	Trachyandesite	AB-T	This paper	
094	25°43′02″ S/56°54′33″ W	140/89	0.15	Phonotephrite	B-P	This paper	
095	25°43′004″ S/56°54′32″ W	320/89	0.35	Tephriphonolite	B-P	[8, 21, 36]	
096	25°43′04″ S/56°54′36″ W	320/89	3.00	Phonotephrite	B-P	This paper	
097	25°43′25″ S/56°56′40″ W	300/89	0.20	Tephrite	B-P	[8, 21, 36]	
098	25°43′30″ S/56°56′41″ W	310/89	0.35	Tephrite	B-P	[8, 21, 36]	
099	25°43′37″ S/56°56′43″ W	250/89	0.80	Peralk. Phon.	B-P	This paper	
100	25°43′39″ S/56°56′40″ W	130/89	0.35	Phonotephrite	B-P	This paper	

Table 1: Continued.

Field number	Latitude/Longitude	Dip direction	Width (m)	Rock	Evolutive trend	References	Chronology
101	25°43′41″ S/56°56′37″ W	140/89	0.20	Phonotephrite	B-P	This paper	
102	25°43′59″ S/56°54′29″ W	300/89	0.60	Trachyphonolite	AB-T	This paper	
103	25°44′02″ S/56°54′35″ W	125/89	1.25	Peralk. Phon.	B-P	[8, 21, 36]	
104	25°43′13″ S/56°54′44″ W	125/89	0.40	Trachyphonolite	AB-T	[8, 21, 36]	
105	25°44′13″ S/56°54′24″ W	120/89	0.25	Tephriphonolite	B-P	[8, 21, 36]	
106	25°44′13″ S/56°54′24″ W	155/89	2.00	Tephrite	B-P	This paper	
107	25°44′17″ S/56°54′36″ W	125/89	1.80	Trachyte	AB-T	This paper	
108	25°44′35″ S/56°55′07″ W	345/89	0.70	Tephriphonolite	B-P	This paper	
109	25°44′40″ S/56°55′10″ W	160/89	1.00	Tephrite	B-P	This paper	109 is cut by 110
110	25°44′40″ S/56°55′10″ W	345/89	3.20	Phonolite	B-P	This paper	
111	25°46′26″ S/56°56′17″ W	295/89	1.60	Tephriphonolite	B-P	This paper	
112	25°47′06″ S/56°56′14″ W	170/89	2.60	Peralk. Phon.	B-P	This paper	
113	25°47′39″ S/56°56′18″ W	305/89	3.20	Phonotephrite	B-P	This paper	
114	25°47′42″ S/56°56′16″ W	345/89	0.55	Phonolite	B-P	This paper	
115	25°47′44″ S/56°56′18″ W	130/89	8.00	Trachyphonolite	AB-T	This paper	
116	25°47′46″ S/56°56′20″ W	155/89	0.40	Phonolite	B-P	[8, 21, 36]	
117	25°47′46″ S/56°56′19″ W	330/89	0.25	Tephriphonolite	B-P	[8, 21, 36]	
118	25°47′46″ S/56°56′19″ W	150/89	2.50	Phonolite	B-P	This paper	
119	25°48′04″ S/56°56′22″ W	315/89	1.70	Tephriphonolite	B-P	This paper	
120	25°48′27″ S/56°56′0/5″ W	125/89	0.35	Trachyandesite	AB-T	[8, 21, 36]	
121	25°50′43″ S/56°56′22″ W	155/89	1.20	Phonolite	B-P	This paper	
122	25°48′45″ S/56°56′30″ W	340/89	2.70	Phonolite	B-T	This paper	
123	25°51′28″ S/56°55′37″ W	160/89	0.80	Tephrite	B-P	This paper	
124	25°47′37″ S/56°57′05″ W	160/89	0.60	Phonolite	B-P	This paper	
125	25°47′45″ S/56°57′06″ W	125/89	2.40	Tephriphonolite	B-P	This paper	
126	25°47′45″ S/56°57′04″ W	320/89	1.80	Trachyandesite	AB-T	This paper	
127	25°47′57″ S/56°57′10″ W	330/89	1.00	Phonotephrite	B-P	This paper	
128	25°47′59″ S/56°57′12″ W	310/89	0.20	Tephrite	B-P	This paper	
129	25°48′43″ S/56°57′091″ W	315/89	0.35	Tephrite	B-P	This paper	
130	25°48′45″ S/56°57′11″ W	340/89	2.70	Peralk. Phon.	B-P	This paper	
131	25°48′45″ S/56°57′11″ W	300/89	0.25	Trachyphonolite	AB-T	[8, 21, 36]	
132	25°48′43″ S/56°57′09″ W	150/89	0.35	Peralk. Phon.	B-P	This paper	
133	25°49′53″ S/56°57′43″ W	330/89	0.20	Peralk. Phon.	B-P	This paper	
134	25°49′53″ S/56°57′43″ W	030/89	0.70	Trachyte	AB-T	This paper	134 is cut by 133
135	25°49′53″ S/56°57′43″ W	150/89	0.35	Phonotephrite	B-T	[8, 21, 36]	
136	25°49′55″ S/56°57′40″ W	070/89	0.20	Phonolite	B-P	This paper	
137	25°47′55″ S/56°57′53″ W	140/89	0.40	Tephrite	B-P	This paper	
138	25°48′00″ S/56°57′55″ W	300/89	1.30	Trachyandesite	AB-T	This paper	
139	25°47′45″ S/56°57′29″ W	165/89	3.00	Tephriphonolite	B-P	This paper	
140	25°47′25″ S/56°57′39″ W	135/89	0.70	Trachyphonolite	AB-T	This paper	
141	25°47′30″ S/56°57′20″ W	155/89	0.35	Peralk. Phon.	B-P	This paper	
142	25°47′32″ S/56°57′30″ W	31/89	0.35	Trachyandesite	AB-T	[8, 21, 36]	
143	25°47′32″ S/56°57′28″ W	165/89	1.50	Phonolite	B-P	This paper	
144	25°47′30″ S/56°57′25″ W	335/89	0.25	Tephrite	B-P	This paper	
145	25°47′27″ S/56°57′26″ W	115/89	1.60	Trachyte	AB-T	This paper	
146	25°47′27″ S/56°57′26″ W	120/89	0.35	Tephriphonolite	B-P	[8, 21, 36]	
147	25°47′19″ S/56°57′35″ W	160/89	0.35	Phonolite	AB-T	This paper	
148	25°47′29″ S/56°57′30″ W	305/89	0.25	Trachyphonolite	AB-T	This paper	
149	25°47′30″ S/56°57′25″ W	330/89	0.40	Tephrite	B-P	[8, 21, 36]	
150	25°47′35″ S/56°57′23″ W	345/89	2.30	Phonolite	B-P	This paper	

Table 1: Continued.

Field number	Latitude/Longitude	Dip direction	Width (m)	Rock	Evolutive trend	References	Chronology
151	25°43′37″ S/56°53′19″ W	240/89	0.80	Phonolite	B-P	This paper	
152	25°44′26″ S/56°51′17″ W	135/89	10.0	Phonolite	B-P	[8, 21, 36]	
153	25°44′28″ S/56°51′30″ W	295/89	0.80	Trachyte	AB-T	[8, 21, 36]	
154	25°44′30″ S/56°51′25″ W	330/89	0.45	Peralk. Phon.	B-P	This paper	
155	25°44′07″ S/56°52′08″ W	120/89	3.00	Phonotephrite	B-P	This paper	
156	25°44′09″ S/56°52′10″ W	310/89	2.70	Tephriphonolite	B-P	This paper	
157	25°44′11″ S/56°52′12″ W	335/89	1.20	Peralk. Phon.	B-P	This paper	
158	25°44′09″ S/56°52′23″ W	340/89	0.30	Peralk. Phon.	B-P	[8, 21, 36]	
159	25°44′10″ S/56°52′20″ W	330/89	0.20	Phonotephrite	B-P	[8, 21, 36]	
160	25°44′15″ S/56°52′15″ W	115/89	0.45	Trachyphonolite	AB-T	[8, 21, 36]	
161	25°44′16″ S/56°52′18″ W	130/89	0.20	Phonotephrite	B-P	[8, 21, 36]	
162	25°44′17″ S/56°52′20″ W	155/89	0.35	Phonolite	B-P	This paper	
163	25°45′17″ S/56°52′05″ W	320/89	0.20	Tephrite	B-P	This paper	
164	25°46′01″ S/56°52′18″ W	320/89	0.60	Phonolite	B-P	This paper	
165	25°46′01″ S/56°52′18″ W	115/89	1.00	Tephrite	B-P	This paper	165 is cut by 164
166	25°46′14″ S/56°52′25″ W	125/89	2.30	Tephrite	B-P	This paper	
167	25°46′18″ S/56°52′19″ W	330/89	0.90	Peralk. Phon.	B-P	This paper	
168	25°46′20″ S/56°52′23″ W	320/89	0.40	Tephrite	B-P	[8, 21, 36]	
169	25°46′23″ S/56°52′36″ W	120/89	0.30	Trachyte	AB-T	[8, 21, 36]	
170	25°46′25″ S/56°52′34″ W	340/89	0.40	Phonolite	B-P	[8, 21, 36]	
171	25°46′55″ S/56°52′50″ W	320/89	0.25	Tephriphonolite	B-P	[8, 21, 36]	
172	25°46′59″ S/56°52′53″ W	165/89	1.30	Phonolite	AB-T	This paper	
173	25°47′05″ S/56°52′50″ W	340/89	0.35	Phonotephrite	B-P	This paper	
174	25°46′47″ S/56°53′16″ W	295/89	2.40	Trachyphonolite	AB-T	This paper	
175	25°47′04″ S/56°53′03″ W	145/89	1.50	Tephriphonolite	B-P	This paper	
176	25°47′10″ S/56°53′09″ W	170/89	0.20	Peralk. Phon.	B-P	This paper	
178	25°47′14″ S/56°54′01″ W	125/89	0.30	Trachyte	AB-T	[8, 21, 36]	
179	25°46′47″ S/56°53′20″ W	330/89	0.45	Tephrite	B-P	[8, 21, 36]	
180	25°46′49″ S/56°53′28″ W	345/89	2.20	Phonolite	B-P	This paper	
181	25°46′44″ S/56°53′47″ W	325/89	0.50	Tephrite	B-P	This paper	
182	25°46′44″ S/56°53′47″ W	110/89	1.20	Trachyandesite	AB-T	This paper	182 is cut by 181
183	25°45′41″ S/56°48′21″ W	145/89	2.40	Peralk. Phon.	B-P	This paper	
184	25°48′56″ S/56°47′25″ W	075/89	0.80	Phonolite	B-P	This paper	
185	25°48′29″ S/56°48′54″ W	340/89	2.70	Tephriphonolite	B-P	This paper	
186	25°48′53″ S/56°47′05″ W	135/89	0.25	Trachyandesite	AB-T	[8, 21, 36]	
187	25°48′55″ S/56°47′10″ W	150/89	0.40	Tephrite	B-P	[8, 21, 36]	
188	25°48′58″ S/56°47′15″ W	070/89	0.40	Phonolite	B-P	This paper	
189	25°49′10″ S/56°48′50″ W	130/89	0.30	Tephriphonolite	B-P	[8, 21, 36]	
190	25°48′29″ S/56°48′54″ W	115/89	1.80	Trachyte	AB-T	This paper	
191	25°48′32″ S/56°52′52″ W	120/89	0.35	Tephrite	B-P	This paper	
192	25°48′49″ S/56°52′50″ W	130/89	0.40	Phonolite	B-T	This paper	
193	25°48′59″ S/56°52′55″ W	280/89	1.30	Trachyphonolite	AB-T	This paper	
194	25°49′02″ S/56°52′50″ W	150/89	0.35	Phonolite	B-P	This paper	
195	25°49′15″ S/56°51′20″ W	320/89	0.20	Phonotephrite	B-P	[8, 21, 36]	
196	25°49′18″ S/56°51′15″ W	140/89	0.80	Phonolite	B-P	This paper	
197	25°49′14″ S/56°53′09″ W	330/89	3.00	Tephrite	B-P	This paper	
198	25°49′10″ S/56°53′22″ W	320/89	0.20	Phonolite	B-P	[8, 21, 36]	
199	25°48′40″ S/56°48′32″ W	315/89	0.40	Trachyandesite	AB-T	[8, 21, 36]	
200	25°49′37″ S/56°53′24″ W	160/89	0.25	Peralk. Phon.	B-P	This paper	

Table 1: Continued.

Field number	Latitude/Longitude	Dip direction	Width (m)	Rock	Evolutive trend	References	Chronology
201	25°49′38″ S/56°53′04″ W	310/89	1.80	Trachyphonolite	AB-T	This paper	
202	25°48′09″ S/56°59′10″ W	165/89	1.50	Peralk. Phon.	AB-T	This paper	
203	25°50′40″ S/56°52′47″ W	075/89	0.60	Phonolite	B-P	This paper	
204	25°48′46″ S/56°52′31″ W	145/89	1.00	Tephriphonolite	B-P	This paper	
205	25°47′46″ S/56°52′43″ W	230/89	2.10	Phonotephrite	B-P	This paper	
206	25°47′45″ S/56°52′40″ W	070/89	0.80	Tephrite	B-P	This paper	

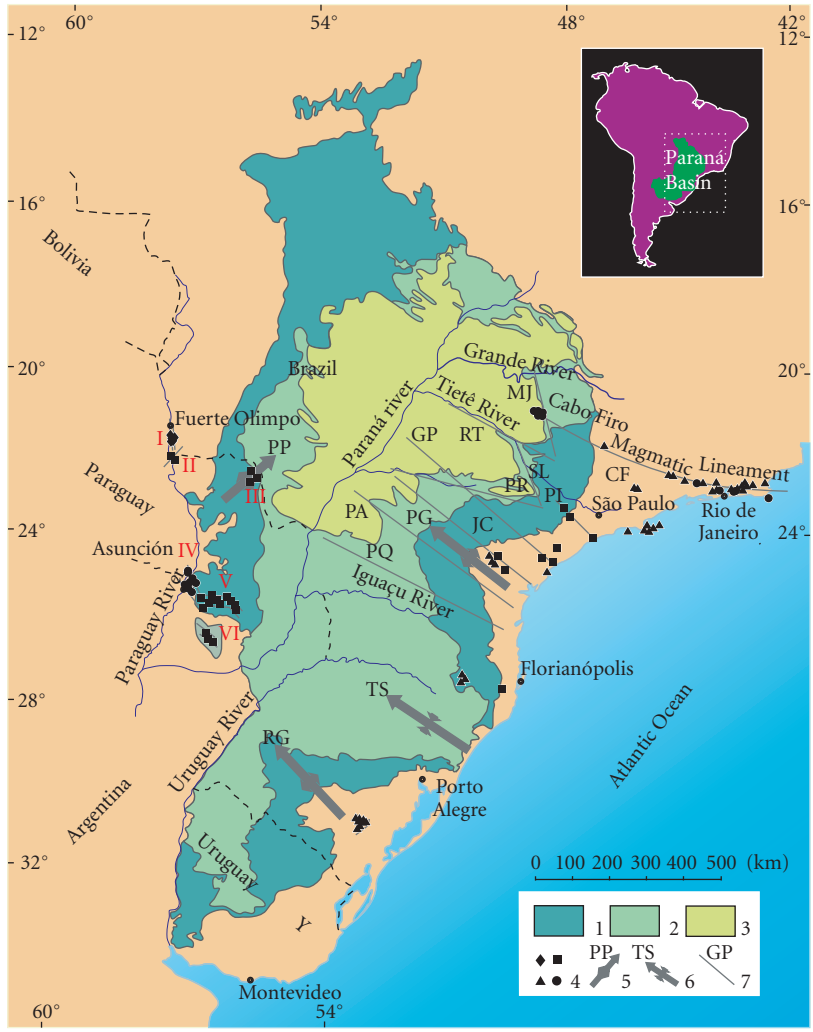

Figure 1: Occurrence of the alkaline intrusions in the southeastern region of the Brazilian Platform and their relationships with major structural features after Riccomini et al. [60]. (1) Late Ordovician to Early Cretaceous Paraná Basin, (2) Early Cretaceous tholeiitic lava-flows, (3) Late Cretaceous Bauru Basin, (4) Age of the alkaline intrusions (diamonds, Permian-Triassic; squares, Early Cretaceous; triangles, Late Cretaceous; circles, Paleogene), (5) Axes of main archs (PG, Ponta Grossa; RG, Rio Grande; PP, Ponta Porã), (6) Torres Syncline, and (7) Major fracture zones (MJ, Moji-Guaçu; CF, Cabo Frio; RT, Rio Tietê; SL, São Carlos-Leme; PR, Paranapanema; PI, Piedade; GP, Guapiara; RA, Rio Alonzo; PQ, Rio Piquiri). Alkaline provinces locations in Paraguay are as follows: I Alto Paraguay; II Rio Apa; III Amambay; IV Asunción; V Central; VI Misiones.

incompatible elements during Proterozoic times. Significant H_2O, CO_2, and F are expected in the mantle source (s) considering the occurrence of coeval carbonatites [7, 18, 32]. Comin-Chiaramonti et al. [26] also suggested that the complex compositional variation registered in the dykes of the Central Province would have resulted from multiple re-equilibrium of the crystallized phases at shallow levels, in a volcanic pressure regime.

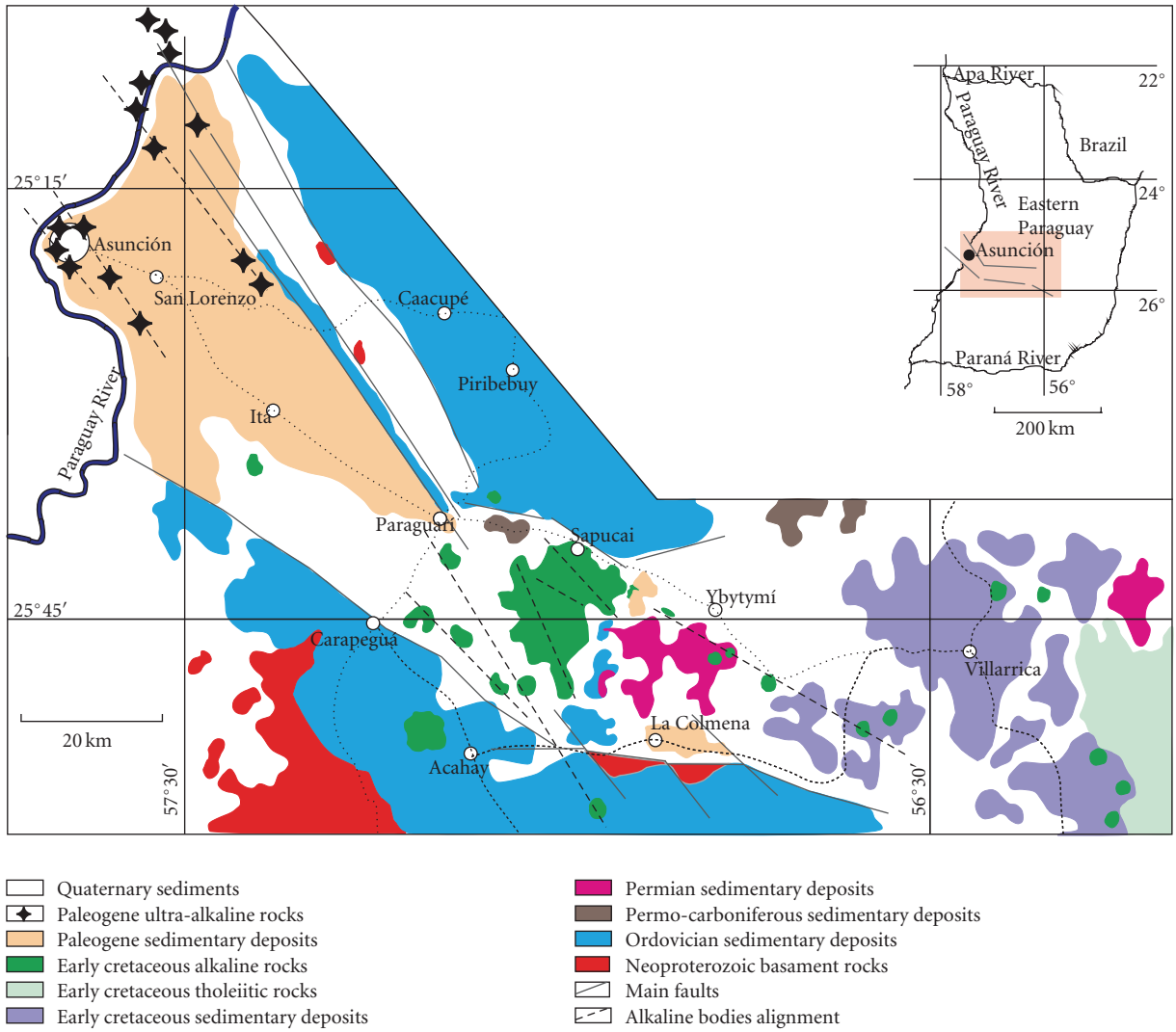

Figure 2: Geological map of the Asunción Rift and associated alkaline occurrences (after Velázquez et al. [17]).

5. Emplacement Ages

The dykes occur associated spatially and temporally with the alkaline lavas, stocks, and plugs. In order to better separate these events, a critical review of the geochronological and paleomagnetic data available in the literature for the dykes will be done following.

The K/Ar whole rock and mineral radiometric ages on a few dykes from the Sapucai area are reported in Velázquez et al. [33] and Gomes et al. [16]. Similar to the data listed in Palmieri [34] and Bitschene [23], these ages display a peak interval between 130–125 Ma. On the other hand, Rb/Sr internal isochron for some intrusive bodies reveal ages of 128 ± 8 Ma and 127 ± 7 Ma [23, 33]. $^{40}Ar/^{39}Ar$ ages determined on phlogopite separates from Sapucai-Villarrica lamprophyre dykes indicate an average value of 127.5 Ma [7].

More recently, a detailed geochronological work using the $^{40}Ar/^{39}Ar$ method was performed by Gomes et al. [35] and Comin-Chiaramonti et al. [10]. The complete set of radiometric data obtained on biotite and plagioclase separates, as well as whole rocks samples, indicate that the dykes and some early alkaline intrusions (stocks and plugs) occur within a time interval of 128–126 Ma, with the latter authors proposing an average value of 126.4 ± 0.4 Ma for the alkaline potassic magmatism of the Central Province.

An extensive paleomagnetic study on the alkaline rocks and associated dykes of the Sapucai region was driven by Ernesto et al. [36]. According to those authors, the dykes acquired two opposite polarities of primary magnetization, normal and reversed, during the emplacement. The cross-cutting intrusion relationships between the dykes indicate that the normal primary magnetizations are younger than reversed.

Although the geochronological data available in the literature for the alkaline potassic magmatism of the Central Province point to wide interval (130–125 Ma), high-precision $^{40}Ar/^{39}Ar$ ages indicate a short period of time (126-127 Ma, cf. [7, 10]). The field evidence suggests that the event would have occurred in a successive way, through

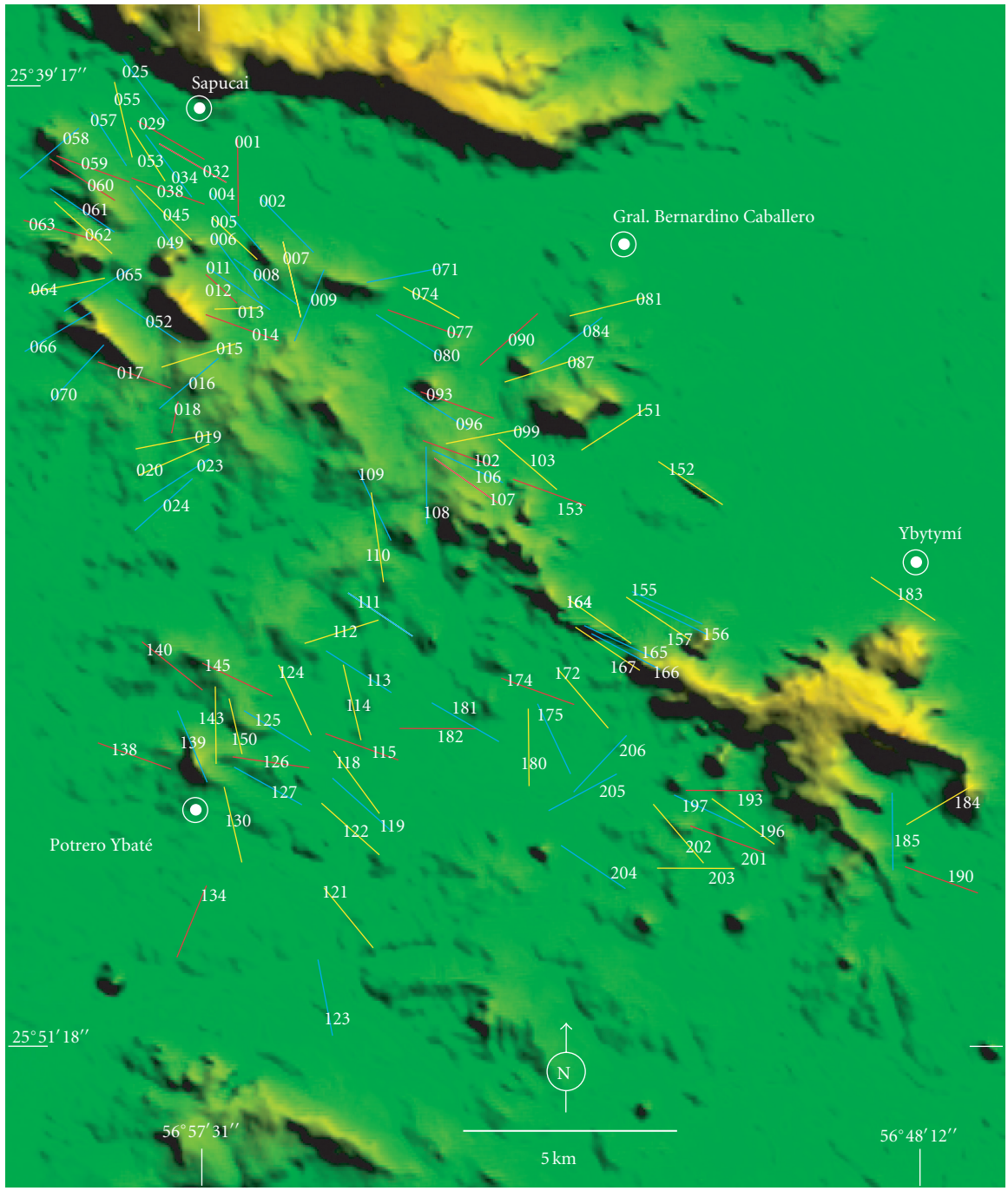

Figure 3: Location map of the alkaline dykes that occur in the central segment of the Asunción Rift. Additional related information is available in Table 1. Dykes with width less than 50 cm are not represented here.

a series of magmatic pulses. The lavas and other major intrusions (ring complexes, plugs, and stocks) predate the dyke intrusions. This fact increases the possibility that all the dyke swarm was formed in a short period of time (less than 1 Ma) and, mainly, during two opposite polarities of primary magnetization, as suggested by the available paleomagnetic data (Figure 5).

6. Orientation of the Dykes and Their Relation with the Regional Structures

Figure 6 shows the orientation of all the dykes measured in the central segment of the Asunción Rift. The measurements refer to dykes with intrusive contacts, showing clear chilled margins in 90% of cases. Two preferential orientations are recognized, NW-SE and NE-SW, the first being more

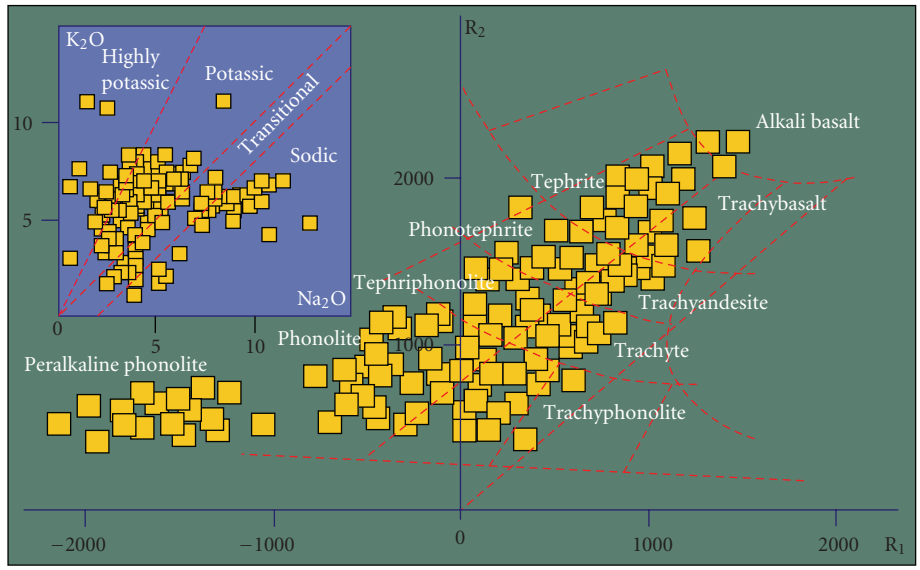

FIGURE 4: Compositional variation in the diagram R_1 (4Si-11Na + K-2Fe + Ti) − R_2 (6Ca + 2Mg + 2Al) (De La Roche et al. [64]) for the alkaline dykes that occur in the central segment of the Asunción Rift. Inset: K_2O versus Na_2O diagram showing the transition between the two series (fields according to [18]). Data source: [8, 26, 31].

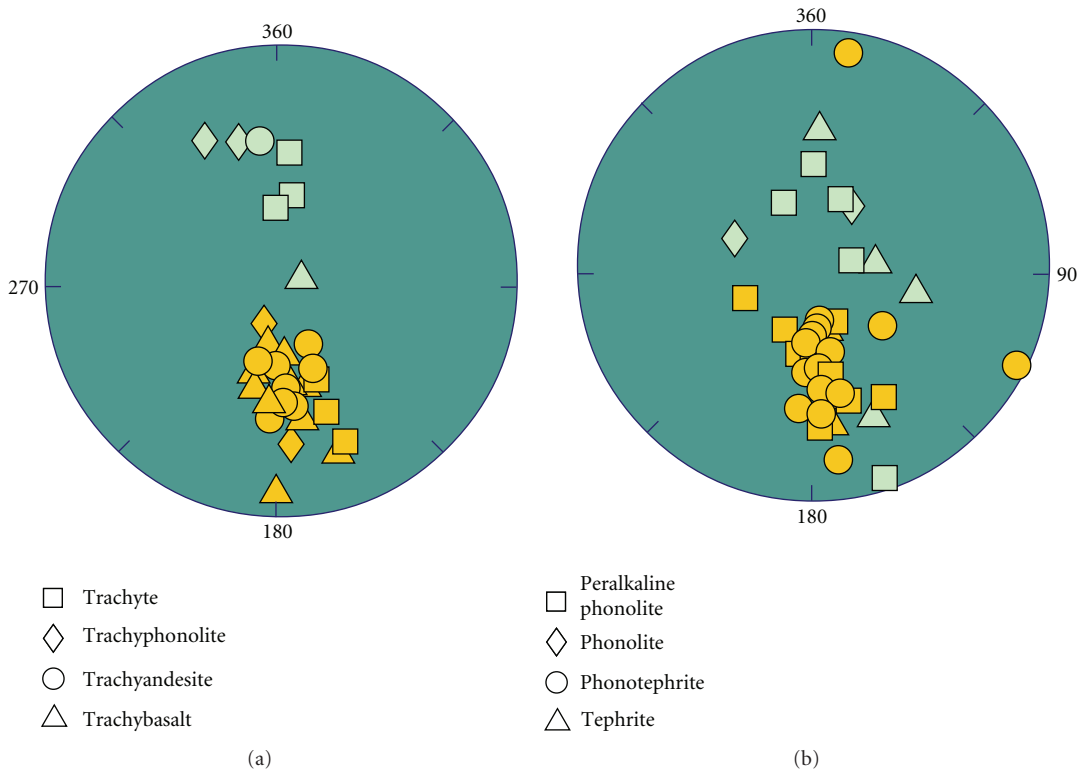

FIGURE 5: Stereographic projection of the site mean paleomagnetic results for the alkaline dykes that occur in the central segment of the Asunción Rift. Note that the majority of the dykes acquired their remanence during a reversed polarity. Data source: [36].

frequent. Interposed between the two main orientations, there are two other less common directions, N-S and E-W. On a regional scale, joint and fault systems of similar orientation also occur. The relative chronology between faults and dykes is not always of easy distinction. In some cases, because the interval between the events was relatively short and, in others, because there was an overlap of events, obliterating the former structure. However, in more favorable outcrops, the structural relationships indicate that the dyke intrusion was preceded by synthetic normal and

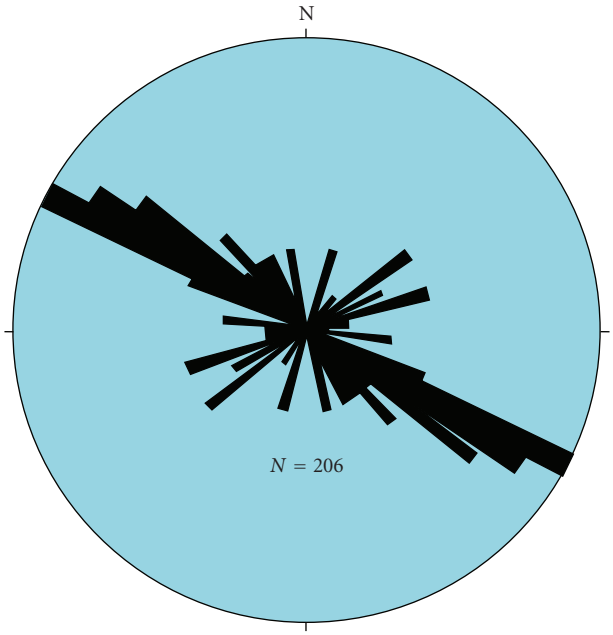

Figure 6: Structural full rose for the alkaline dykes that occur in the central segment of the Asunción Rift.

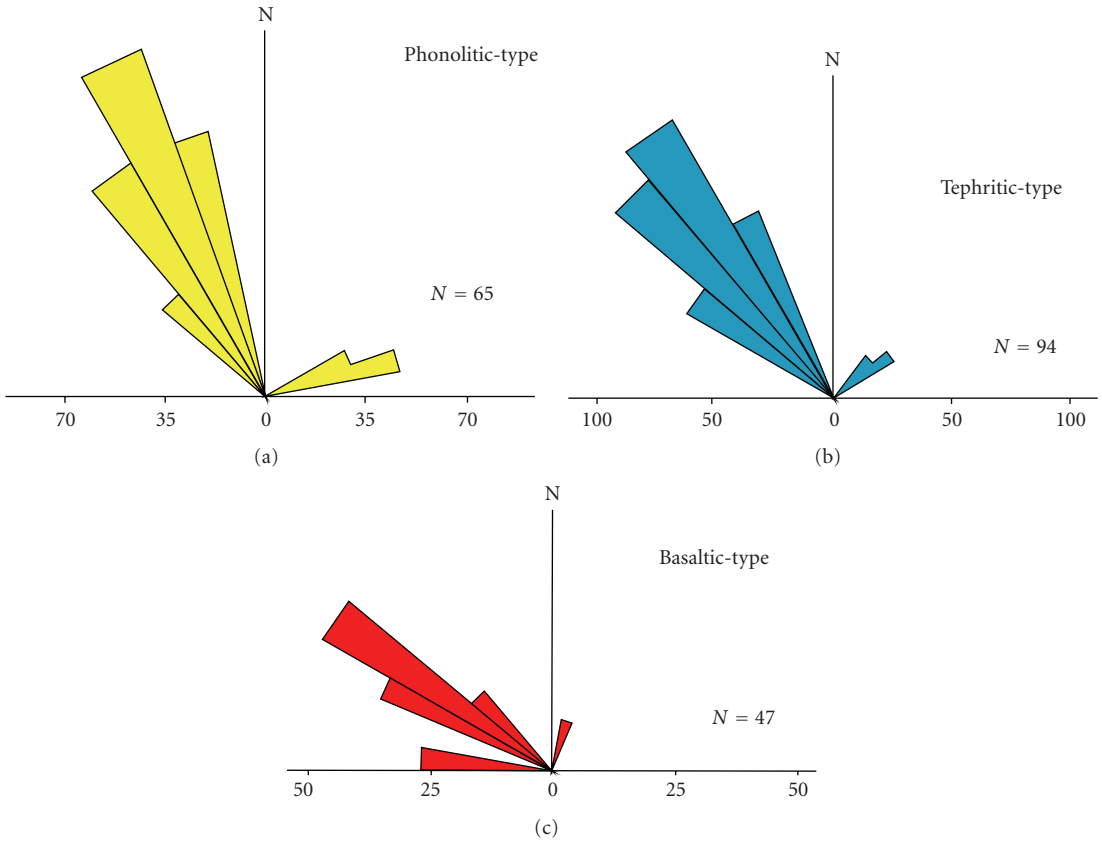

Figure 7: Rose diagrams illustrating the azimuthal orientation for the three main lithological types of alkaline dykes. Note that the mean of the preferential directions indicates a clockwise rotation.

(a) (b) (c)

Figure 8: Field relations illustrating the mechanism of emplacement of the dykes: (a) felsic dyke, with a vertical plane orientated according to N25W, evidencing a normal dilatation, (b) intermediate dyke, orientated according to N35W, showing a normal-oblique separation with slickenside surface on the walls of the dyke, and (c) mafic dyke, orientated according to N50W, showing a typical right-lateral opening with oblique movement between the walls.

some strike-slip faulting. Similarly, the determination of the temporal relation of dyke intrusions was based mainly on their cross-cutting relationships. This correlation indicates that *basaltic-type* predate the *tephritic-type* and both are cut by *phonolitic-type*.

Detailed analysis, combining dyke petrography, orientation pattern, and relative chronology, reveals that the *basaltic-type* is orientated preferentially N50-70W, the *tephritic-type* N30-60W, and the *phonolitic-type* N20-45W (Figure 7). Such disposition shows clearly a rotation from WNW toward NNW during the emplacement of the dykes, accompanied by a progressive compositional change of the magma. Field observations are consistent with continuous extensional deformation and right-lateral rotation, which led to a dynamic interrelation between faulting and dyke injection. The absence of internal solid-state deformation in the dykes and the nature of the kinematic indicators present in the walls suggest that the fault generation and the dyke injection would have occurred simultaneously, under an extensional tectonic regime, followed by a short period of progressive shearing, affecting the walls of the partially solidified dykes (Figure 8).

7. Discussion and Conclusion

The evolution of the regional stress field is frequently determined by structural analyses of faults, fractures, cleavages, and other microtectonic evidence. Unfortunately, these methods do not permit the precise dating of the specific period in which the stress field has been acting. Igneous rocks, however, can be isotopically dated and frequently display distribution and internal structural patterns related to the crustal stress field at the time of magmatism. Therefore, it is possible to establish an absolute chronology of the variation in the trajectory of the regional paleostress-fields [2–5]. This manner, volcanic features are frequently utilized as paleostress indicators, including alignments of volcanoes or ash cones and axes of elongation of volcanic edifices [37, 38].

Dykes are also very important kinematic indicators, considering that magma may invade coeval fractures under the action of a regional paleostress-field [39, 40]. Because magma-driven fracturing is preferentially normal to the principal compressive stress $\sigma 1$ (Anderson's prediction), vertical dykes can only be generated when $\sigma 3$ is horizontal, that is, when the regional paleostress of the crust is dominantly extensional [6, 41–45].

The Cretaceous alkaline dyke swarms of Central-Eastern Paraguay show a large compositional variation, petrographic facies, and texture, offering important constraints on magma generation and dyke intrusions. Field observations indicate that the dykes represent majorly single vertical intrusions, but composite and multiple intrusions are also recognized.

The wide mineralogical variation and heterogeneous geochemical composition of the dykes require a dynamic generation mechanism during their emplacement, with constant and progressive crystal-liquid fractionation from the magmatic chamber. Such rapid rates of magma generation, in short periods of time, argue that partial melting took place during an extensional tectonic regime and by adiabatic decompression. Many of the dykes contain a significant proportion of primary hydrous minerals (biotite and/or amphibole) suggesting that hydrodynamic force (water-vapor pressure) played an important role in the magma generation. As a result of a constant modification of the thermodynamic conditions, the absolute majority of the dykes presents a well-marked change in texture, ranging from holocrystalline to hypocrystalline. In contrast to Komar's prediction [46], no gradual concentration in phenocrysts from the walls to the center or internal structural zoning was observed in those dykes. This fact seems to confirm that flow-differentiation processes were not an important mechanism responsible for their generation. Thus, it is reasonable to admit that the dykes were emplaced in liquid state and consolidated under very fast cooling rates. In this case, an unstable condition of the flow regime due to variables such as the velocity gradient across the fractures, width of the fractures, magma viscosity, cooling rates, and crystal supply caused different effects on the crystals growth during emplacement and broadly influenced textural variations.

Because thin dyke channels may only last for hours to days (cf. [47]), liquids generated in the mantle and subject to continuous removal toward the surface would

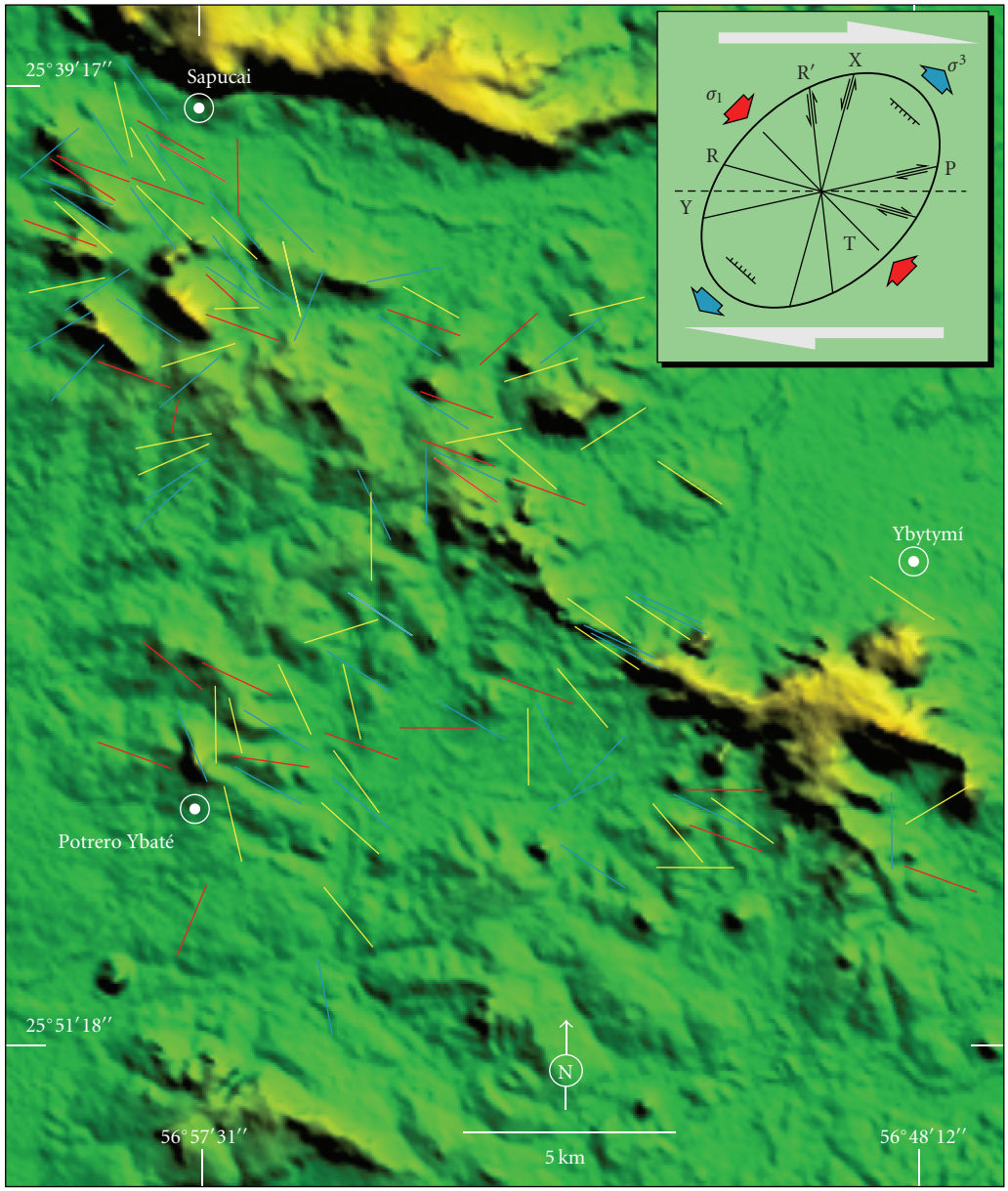

Figure 9: Regional en-échelon distribution and a proposed for the emplacement mechanism of the swarm alkaline dykes (see text for discussion). Schematic Riedel shear model in inset shows theoretical distribution of shear fractures (R, R′, P, X and Y) and tensional fractures (T) in E-W dextral transtensional tectonic regime (cf. [53]). Red and blue arrows indicate shortening axis and extensional axis, respectively. The distinction of dykes is as in Figure 5.

be under the constant influence of the regional stress fields [48–52]. As previously stated, vertical dykes occur as a product of magma-filled fractures when the minimum compressive stress, $\sigma 3$, is perpendicular to the direction of the propagation plane. Such conditions seem to be shown by the field relations of the studied dykes. This assumption is based on the careful examination of the chilled margins of the dykes and their geochemical data, which indicate no obvious significant interaction with the country rocks during magma injection. The walls of the dykes usually display normal dilatation and planar morphology. Only a few bodies show oblique opening, in either a dextral or sinistral sense, with overall extension preferentially orthogonal to the main propagation trajectory of the dykes. Additional evidence, such as the limited length (less than 3 km) and narrow width (average of 1–3 m) of the sheet-like bodies, the lack of a flux orientation of phenocrysts aligned parallel at the dyke margins, and the en-échelon regional distribution, indicates that vertical injection was more common than lateral magma injection.

The regional N20-70W-trending of the Cretaceous alkaline dykes suggests that the opening fractures and the magma injection were not perturbed significantly by pre-existing lines of weakness in the country rocks. Therefore, the well-expressed structural fingerprints of the dykes indicate an overall remote stress regime characterized by a NW-trending

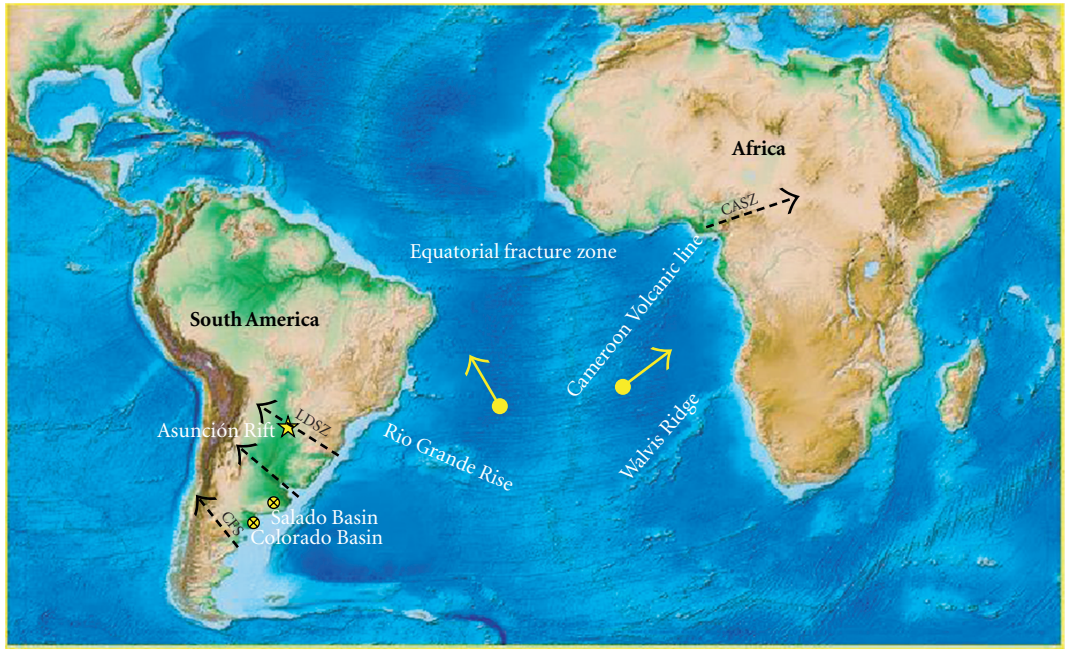

Figure 10: Schematic map showing the main larger deformation areas that occurred during the phase of continental breakup. Dashed black arrows: larger dextral shear zone (LDSZ), Gastre fault system (GFS), and central African sinestral shear zone (CASZ). Yellow arrows indicate the plate motion according to Fairhead and Wilson [65]. Note that the Asunción Rift is closely related to the LDSZ. Copyrights of the map for National Geophysical Data Center.

maximum horizontal shortening axis, an NE-oriented maximum horizontal extension axis, and vertical intermediate stress. Slickenside lineation analysis on NNW-sinestral and WNW-dextral conjugate strike-slip faults plane that outline the central segment borders of Asunción Rift (Figure 2) is also compatible with this paleostress orientation [19, 20, 22]. Basic criteria, such as the geometry, the orientation, and distribution pattern and the relative chronology of the dykes and regional faults, are widely consistent with an E-W dextral transtensional tectonic regime (Figure 9). In the context of a simple Riedel shear model [53], the *basaltic-type* dykes were preferentially injected along R fractures during the initial stage of the deformation. Some *tephitic-type* dykes also filled in part these fractures. With strain increase, R′ followed by P fractures were generated, which served as conduits for the *tephitic-type* dykes. Isolated occurrences of *phonolitic-type* dykes display consistent orientation with this phase of deformation. At an advanced stage of strain, finally, T fractures, perpendicular to the maximum extension axis, and Y fractures, parallel to the principal displacement zone direction, controlled the intrusion of the *phonolitic-type* dykes. Pattern orientation corresponding to X fractures is relatively uncommon in the study area. Assuming that the dykes were injected during an event of progressive deformation, the regional distribution in right- and left-stepping en-échelon corresponds to shear fractures (R, R′ and P) and tensional fractures (T). This framework structural has significant implications with regard to the right-lateral global rotation during dyke intrusions. The local parallel orientation of composite and multiple dykes confirm that the trajectory of the regional paleostress fields was relatively constant at the time of the dyke intrusion.

The relationship between alkaline magmatism associated with the Asunción Rift and basaltic melt generation in the Paraná-Etendeka large igneous province is well recognized [7–9]. Several geological evidence suggest that this episode of instability was occasioned by the lithospheric extension, continental breakup, and mantle plume, provoking a wide range of structural discontinuities, the installation of new sedimentary basins, and the intrusion of numerous alkaline bodies [8, 54–56]. High-precision $^{40}Ar/^{39}Ar$ age determinations indicate that the alkaline magmatism in Eastern Paraguay can be grouped in two main events. The early stage (~145 and 138.9 Ma, cf. [7, 10]), located in the north region of the country, was before the first eruption of the flood basalts at 133 Ma (cf. [14, 15]) and a late phase (~127 and 126.4 Ma), concentrated in the Asunción Rift, which coincides with the youngest flood basalts that occur near the Brazilian and Uruguayan shoreline [7, 10]. In terms of petrogenetic evolution, the Paraná-Etendeka large igneous province and associated alkaline intrusive rocks are commonly interpreted as derived from a similar mantle source region by upwelling Tristan plume [57–59]. Gibson et al. [7] postulated that the late event (~127 Ma) of Paraguayan alkaline magmatism would be associated with the final phase of the opening of the South Atlantic Ocean. According to Riccomini et al. [60] and Comin-Chiaramonti et al. [10], the regional spatial distribution of the Cretaceous and Tertiary alkaline magmatism along the coast lines of the South Atlantic continental margins and West Africa reveal that major dextral and sinestral shear zones exerted significant control on the alkaline bodies alignment. This evidence suggests an analogous intraplate deformation in both South American and African plates, as previously proposed by Vink

[61] and Fairhead [39]. In this context, a lateral perturbation of the regional stress intensity induced by the differential motion of the plates at the time of continental breakup would favor the propagation of brittle structures toward the interior of the continents (Figure 10). Finally, the presence of a dextral strike-slip motion along the South American second-order plate boundary, proposed by Unternehr et al. [62] and N. Eyles and C. H. Eyles [63], the south-eastwards migration of Paraná-Etendeka large igneous province and associated alkaline rocks, suggested by Turner et al. [14] and Gibson et al. [7], and the Cabo Frio magmatic lineament [60] are strongly indicative of a global motion towards WNW of the South American plate, consistent with the pattern of orientation documented for the Cretaceous alkaline dykes of the Asunción Rift.

Acknowledgments

The authors thank Fapesp for financial support (Proc.: 97/01210-4 and Proc. 07/57461-9). They also thank the two anonymous reviewers for their constructive and perceptive commentaries of the manuscript.

References

[1] H. C. Halls and W. F. Fahrig, "Dyke swarms and continental rifting: some concluding remarks," *Geological Association of Canada*, vol. 34, pp. 483–492, 1987.

[2] A. J. Parker, P. C. Rickwood, and D. H. Tucker, *Mafic Dykes and Emplacement Mechanisms*, Balkema, Rotterdam, The Netherlands, 1990.

[3] A. Rubin and D. Pollard, "Dike-induced faulting in rift zones in Iceland and Afar," *Geology*, vol. 16, pp. 413–417, 1998.

[4] D. D. Pollard, "Elementary fracture mechanics applied to the structural interpretation of dykes," in *Mafic Dykes Swarms*, H. H. Halls and W. F. Fahrig, Eds., vol. 4, pp. 5–24, Geological Association of Canada, 1987.

[5] P. T. Delaney, D. D. Pollard, J. I. Ziony, and H. Mckee, "Field relation between dykes and joints: emplacement processes and paleostress analysis," *Journal of Geophysical Research*, vol. 91, pp. 4920–4938, 1986.

[6] E. M. Anderson, *The Dynamics of Faulting and Dyke Formation with Applications to Britain*, Oliver and Boyd, Edinburg, UK, 1951.

[7] S. A. Gibson, R. N. Thompson, and J. A. Day, "Timescales and mechanisms of plume-lithosphere interactions: ^{40}Ar-^{39}Ar geochronology and geochemistry of alkaline igneous rocks from the Paraná-Etendeka large igneous province," *Earth and Planetary Science Letters*, vol. 251, no. 1-2, pp. 1–17, 2006.

[8] P. Comin-Chiaramonti and C. B. Gomes, Eds., *Alkaline Magmatism in Central-Eastern Paraguay. Relationships with Coeval Magmatism in Brazil*, Edusp-Fapesp, São Paulo, Brazil, 1996.

[9] P. Comin-Chiaramonti and C. B. Gomes, Eds., *Mesozoic to Cenozoic Alkaline Magmatism in the Brazilian Platform*, Edusp-Fapesp, São Paulo, Brazil, 2005.

[10] P. Comin-Chiaramonti, A. Marzoli, C. B. Gomes et al., "The origin of post-Paleozoic magmatism in Eastern Paraguay," *Special Paper of the Geological Society of America*, no. 430, pp. 603–633, 2007.

[11] P. R. Renne, M. Ernesto, I. G. Pacca et al., "The age of Paraná flood volcanism, rifting of gondwanaland, and the Jurassic-Cretaceous boundary," *Science*, vol. 258, no. 5084, pp. 975–979, 1992.

[12] P. R. Renne, D. F. Mertz, W. Teixeira, H. Ens, and M. Richards, "Geochronologic constraints on magmatic and tectonic evolution of the Paraná Province," *American Geophysical Union Abstract*, vol. 74, p. 553, 1993.

[13] P. R. Renne, K. Deckart, M. Ernesto, G. Féraud, and E. M. Piccirillo, "Age of the Ponta Grossa dike swarm (Brazil), and implications to Paraná flood volcanism," *Earth and Planetary Science Letters*, vol. 144, no. 1-2, pp. 199–211, 1996.

[14] S. Turner, M. Regelous, S. Kelley, C. Hawkesworth, and M. Mantovani, "Magmatism and continental break-up in the South Atlantic: high precision ^{40}Ar-^{39}Ar geochronology," *Earth and Planetary Science Letters*, vol. 121, no. 3-4, pp. 333–348, 1994.

[15] K. Stewart, S. Turner, S. Kelley, C. Hawkesworth, L. Kirstein, and M. Mantovani, "3-D, ^{40}Ar-^{39}Ar geochronology in the Paraná continental flood basalt province," *Earth and Planetary Science Letters*, vol. 143, no. 1–4, pp. 95–109, 1996.

[16] C. B. Gomes, P. Comin-Chiaramonti, V. F. Velázquez, and D. Orué, "Alkaline magmatism in Paraguay: a review," in *Alkaline Magmatism in Central-Eastern Paraguay. Relationships with Coeval Magmatism in Brazil*, P. Comin-Chiaramonti and C. B. Gomes, Eds., pp. 31–56, Edusp-Fapesp, São Paulo, Brazil, 1996.

[17] V. F. Velázquez, C. B. Gomes, D. Orué, and P. Comin-Chiaramonti, "Magmatismo alcalino do Paraguai: uma revisão e atualização das províncias," *Boletim do Instituto de Geociências*, vol. 27, pp. 61–79, 1996.

[18] P. Comin-Chiaramonti, A. Cundari, E. M. Piccirillo et al., "Potassic and sodic igneous rocks from Eastern Paraguay: their origin from the lithospheric mantle and genetic relationships with the associated Paraná flood tholeiites," *Journal of Petrology*, vol. 38, no. 4, pp. 495–528, 1997.

[19] V. F. Velázquez, C. Riccomini, C. B. Gomes, L. Figueredo, and C. Figueredo, "Relações tectônicas do magmatismo alcalino do Paraguai Oriental," *Revista do Instituto Geológico*, vol. 19, pp. 41–48, 1998.

[20] C. Riccomini, V. F. Velázquez, and C. B. Gomes, "Cenozoic lithospheric faulting in the Asunción Rift, eastern Paraguay," *Journal of South American Earth Sciences*, vol. 14, no. 6, pp. 625–630, 2001.

[21] J. M. DeGraff, "Late Mesozoic crustal extension and rifting on the western of the Paraná Basin, Paraguay," *Geological Society of America*, vol. 17, p. 560, 1985.

[22] C. Riccomini, V. F. Velázquez, C. B. Gomes, A. Milan, and A. E. M. Sallun, "The tectonic evolution of the Asunción Rift, Eastern Paraguay," *Anais da Academia Brasileira de Ciências*, vol. 74, p. 555, 2002.

[23] P. Bitschene, *Mesozoischer und Kanozoischer anorogener magmatismus in Ostparaguay: arbeiten zur geologie und petrologie zweier Alkaliprovinzen*, Ph.D. Dissertation, Heidelberg University, Heidelberg, Germany, 1987.

[24] J. Berrocal and C. Fernandes, "Seismicity in Paraguay and neighbouring regions," in *Alkaline Magmatism in Central-Eastern Paraguay, Relationships with Coeval Magmatism in Brazil*, P. Comin-Chiaramonti and C. B. Gomes, Eds., pp. 57–66, Edusp-Fapesp, São Paulo, Brazil, 1996.

[25] K. L. Hegarty, I. R. Duddy, and P. F. Green, "The thermal history in around the Paraná basin using apatite fission track analysis—implications for hydrocarbon occurrences and basin formation," in *Alkaline Magmatism in Central-Eastern*

Paraguay, Relationships with Coeval Magmatism in Brazil, P. Comin-Chiaramonti and C. B. Gomes, Eds., pp. 67–84, Edusp-Fapesp, São Paulo, Brazil, 1996.

[26] P. Comin-Chiaramonti, A. Cundari, C. B. Gomes et al., "Potassic dyke swarm in the Sapucai Graben, eastern Paraguay: petrographical, mineralogical and geochemical outlines," *Lithos*, vol. 28, no. 3–6, pp. 283–301, 1992.

[27] P. Comin-Chiramonti, A. Cundari, C. B. Gomes et al., "Mineral chemistry and its genetic significance of major and accessory mineral from a potassic dyke swarm in the Sapucai Graben, central-eastern Paraguay," *Geochimica Brasiliensis*, vol. 4, pp. 175–206, 1990.

[28] P. Comin-Chiramonti, A. Cundari, A. De Min, C. B. Gomes, and V. F. Velázquez, "Magmatism in Eastern Paraguay: occurrence and petrography," in *Alkaline Magmatism in Central-Eastern Paraguay. Relationships with Coeval Magmatism in Brazil*, P. Comin-Chiaramonti and C. B. Gomes, Eds., pp. 103–122, Edusp-Fapesp, São Paulo, Brazil, 1996.

[29] M. D. Druecker and S. P. Gay Jr., "Mafic dyke swarms associated with Mesozoic rifting in eastern Paraguay, South America," *Geological Association of Canada*, vol. 34, pp. 187–193, 1987.

[30] A. Cundari and P. Comin-Chiaramonti, "Mineral chemistry of alkaline rocks from the Asunción-Sapucai graben (Central-Eastern Paraguay)," in *Alkaline Magmatism in Central-Eastern Paraguay. Relationships with Coeval Magmatism in Brazil*, P. Comin-Chiaramonti and C. B. Gomes, Eds., pp. 181–193, Edusp-Fapesp, São Paulo, Brazil, 1996.

[31] C. B. Gomes, P. Comin-Chiaramonti, A. De Min et al., "Atividade filoniana associada ao complexo alcalino de Sapukai, Paraguai Oriental," *Geochimica Brasiliensis*, vol. 3, pp. 93–114, 1989.

[32] A. Castorina, R. Petrini, P. Comin-Chiaramonti, G. Capaldi, and G. Pardini, "Potassic magmatism from the Asunción-Sapucai graben, Eastern Paraguay: inferences on mantle sources by Sr-Nd isotopic systematics," in *Alkaline Magmatism in Central-Eastern Paraguay. Relationships with Coeval Magmatism in Brazil*, P. Comin-Chiaramonti and C. B. Gomes, Eds., pp. 195–206, Edusp-Fapesp, São Paulo, Brazil, 1996.

[33] V. F. Velázquez, C. B. Gomes, and G. Capaldi, "Magmatismo alcalino Mesozóico na porção centro oriental do Paraguai: aspectos geocronológicos," *Geochimica Brasiliensis*, vol. 6, pp. 23–35, 1992.

[34] J. H. Palmieri, *El complejo alcalino de Sapukai (Paraguay Oriental)*, Ph.D. Dissertation, University of Salamanca, Salamanca, Spain, 1973.

[35] C. B. Gomes, A. Milan, and V. F. Velázquez, "Magmatismo alcalino na porção centro-oriental do Paraguai: novos dados geocronológicos para as rochas das Províncias Central e Assunção," in *Proceedings of the 7th Congresso de Geoquímica dos países de língua portuguesa*, vol. 1, pp. 179–183, Revista da Faculdade de Ciências, Universidade Eduardo Mondlane, Maputo, Moçambique, 2003.

[36] M. Ernesto, P. Comin-Chiaramonti, C. B. Gomes, and J. C. Velázquez, "Paleomagnetic data from the central alkaline province, Eastern Paraguay," in *Alkaline Magmatism in Central-Eastern Paraguay. Relationships with Coeval Magmatism in Brazil*, P. Comin-Chiaramonti and C. B. Gomes, Eds., vol. 123, pp. 238–253, Edusp-Fapesp, São Paulo, Brazil, 1996.

[37] E. D. Jackson and H. R. Shaw, "Stress pattern in central portion of the pacific plate delineated in time by linear volcanic chains," *Journal of Geophysical Research*, vol. 80, pp. 1816–1874, 1975.

[38] G. Féraud, C. Giannérini, and R. Camprendon, "Dyke swarms as paleostress indicators in areas adjacent to continental collision zones: examples from the European and northwest Arabian plates," *Geological Association of Canada*, vol. 34, pp. 273–278, 1987.

[39] J. D. Fairhead, "Mesozoic plate tectonic reconstructions of the central South Atlantic Ocean: the role of the West and Central African rift system," *Tectonophysics*, vol. 155, no. 1–4, pp. 181–191, 1988.

[40] A. F. Glazner, J. M. Bartley, and B. S. Carl, "Oblique opening and noncoaxial emplacement of the Jurassic Independence dike swarm, California," *Journal of Structural Geology*, vol. 21, no. 10, pp. 1275–1283, 1999.

[41] J. R. Lister, "Fluid-mechanical models of crack propagation and their application to magma transport in dykes," *Journal of Geophysical Research*, vol. 96, no. 6, p. 10, 1991.

[42] W. F. Fahrig, K. W. Christie, E. H. Chown, D. Janes, and N. Machado, "The tectonic significance of some basic dyke swarms in the Canadian Superior province with special reference to the geochemistry and paleomagnetism of the Mistassini swarm, Quebec, Canada," *Canadian Journal of Earth Sciences*, vol. 23, no. 2, pp. 238–253, 1986.

[43] W. F. Fahrig, "The tectonic setting of continental mafic dyke swarms: failed arm and early passive margin," *Geological Association of Canada*, vol. 34, pp. 331–348, 1987.

[44] R. E. Ernst, E. B. Grosfils, and D. Mège, "Giant dike swarms: earth, Venus, and Mars," *Annual Review of Earth and Planetary Sciences*, vol. 29, pp. 489–534, 2001.

[45] G. Hou, T. M. Kusky, C. Wang, and Y. Wang, "Mechanics of the giant radiating Mackenzie dyke swarm: a paleostress field modeling," *Journal of Geophysical Research*, vol. 115, no. 2, Article ID B02402, pp. 1–14, 2010.

[46] P. D. Komar, "Phenocryst interactions and the velocity profile of magma flowing through dikes or sills," *Geological Society American Bulletin*, vol. 83, pp. 1336–1342, 1976.

[47] C. Cadman and J. Tarney, "Intrusion and crystallization features in Proterozoic dyke swarms," in *Mafic Dykes and Emplacement Mechanisms*, A. J. Parker, P. C. Rickwood, and D. H. Tucker, Eds., pp. 13–24, Balkema, Rotterdam, The Netherlands, 1990.

[48] A. Gudmundsson, "Dyke emplacement at divergent plate boundaries," in *Mafic Dykes and Emplacement Mechanisms*, A. J. Parker, P. C. Rickwood, and D. H. Tucker, Eds., pp. 47–62, Balkema, Rotterdam, The Netherlands, 1990.

[49] H. C. Halls, "The importance and potential of mafic dyke swarms in studies of geodynamic processes," *Geoscience Canada*, vol. 9, no. 3, pp. 145–154, 1982.

[50] W. R. A. Baragar, R. E. Ernst, L. Hulbert, and T. Peterson, "Longitudinal petrochemical variation in the Mackenzie dyke swarm, Northwestern Canadian shield," *Journal of Petrology*, vol. 37, no. 2, pp. 317–359, 1996.

[51] E. B. Grosfils and J. W. Head, "The global distribution of giant radiating dike swarms on Venus: implications for the global stress state," *Geophysical Research Letters*, vol. 21, no. 8, pp. 701–704, 1994.

[52] A. Gudmundsson, "Surface stresses associated with arrested dykes in rift zones," *Bulletin of Volcanology*, vol. 65, no. 8, pp. 606–619, 2003.

[53] G. Dresen, "Stress distribution and the orientation of Riedel shears," *Tectonophysics*, vol. 188, no. 3-4, pp. 239–247, 1991.

[54] F. F. M. D. Almeida, B. B. D. Brito Neves, and C. D. R. Carneiro, "The origin and evolution of the South American platform," *Earth Science Reviews*, vol. 50, no. 1-2, pp. 77–111, 2000.

[55] D. Peate, "The Parana-Etendeka Province," in *Large Igneuos Province: Continetal, Oceanic, Planetary Flood Volcanism*, J. Mahoney and M. F. Coffin, Eds., pp. 217–245, American Geophyscial Union, Washington, DC, USA, 1992.

[56] C. J. Hawkesworth, "Paraná magmatism and the opening of the South Atlantic," *Geological Society of London Special Publication*, vol. 68, pp. 221–240, 1992.

[57] A. Ewart, S. C. Milner, R. A. Armstrong, and A. R. Duncan, "Etendeka volcanism of the Goboboseb Mountains and Messum Igneous Complex, Namibia. Part I: geochemical evidence of early cretaceous Tristan plume melts and the role of crustal contamination in the Paraná-Etendeka CFB," *Journal of Petrology*, vol. 39, no. 2, pp. 191–225, 1998.

[58] S. A. Gibson, R. N. Thompson, O. H. Leonardos, A. P. Dickin, and J. G. Mitchell, "The limited extent of plume-lithosphere interactions during continental flood-basalt genesis: geochemical evidence from Cretaceous magmatism in southern Brazil," *Contributions to Mineralogy and Petrology*, vol. 137, no. 1-2, pp. 147–169, 1999.

[59] R. N. Thompson, S. A. Gibson, A. P. Dickin, and P. M. Smith, "Early cretaceous basalt and picrite dykes of the Southern Etendeka Region, NW Namibia: windows into the role of the Tristan mantle plume in Paraná-Etendeka magmatism," *Journal of Petrology*, vol. 42, no. 11, pp. 2049–2081, 2001.

[60] C. Riccomini, V. F. Velázquez, and C. B. Gomes, "Tectonic controls of the Mesozoic and Cenozoic alkaline magmatism in central-southeastern Brazilian Platform," in *Mesozoic to Cenozoic Alkaline Magmatism in the Brazilian Platform*, P. Comin-Chiaramonti and C. B. Gomes, Eds., vol. 123, pp. 31–56, Edusp-Fapesp, São Paulo, Brazil, 2005.

[61] G. E. Vink, "Continental rifting and the implications for plate tectonic reconstructions," *Journal of Geophysical Research*, vol. 87, no. 13, pp. 10677–10688, 1982.

[62] P. Unternehr, D. Curie, J. L. Olivet, J. Goslin, and P. Beuzart, "South Atlantic fits and intraplate boundaries in Africa and South America," *Tectonophysics*, vol. 155, no. 1–4, pp. 169–179, 1988.

[63] N. Eyles and C. H. Eyles, "Glacial geologic confirmation of an intraplate boundary in the Parana basin of Brazil," *Geology*, vol. 21, no. 5, pp. 459–462, 1993.

[64] H. De La Roche, J. Leterrier, P. Grancalude, and M. Marchal, "A classification of volcanic and plunotic rocks using R1-R2 diagram and major elements analyses. Its relationship with currents nomenclature," *Chemical Geology*, vol. 29, pp. 183–210, 1980.

[65] J. D. Fairhead and M. Wilson, "Sea-floor spreading and deformation processes in the South Atlantic Ocean: are hot spots needed?" 2004, http://www.mantleplumes.org/SAtlantic.html.